JOURNAL OF PETROLOGY | VOLUME 39 | NUMBER 11 & 12 | PAGES 1953–1964 | 1998

The Continuum of Primary Carbonatitic–Kimberlitic Melt Compositions in Equilibrium with Lherzolite: Data from the System $CaO–MgO–Al_2O_3–SiO_2–CO_2$ at 6 GPa

JOHN A. DALTON* AND DEAN C. PRESNALL

MAGMALOGY LABORATORY, DEPARTMENT OF GEOSCIENCES, UNIVERSITY OF TEXAS AT DALLAS, RICHARDSON, TX 75083, USA

RECEIVED SEPTEMBER 30, 1997; REVISED TYPESCRIPT ACCEPTED JUNE 12, 1998

The compositions of liquids in equilibrium with lherzolite over a range of temperatures (1380–1505°C) above the carbonated lherzolite solidus have been determined in the system CaO–MgO–Al_2O_3–SiO_2–CO_2 at 6 GPa. Melt compositions show systematic variation with temperature from carbonatitic (Mg/Ca ratio 1; 5 wt % SiO_2) at the solidus (1380°C) through intermediary compositions to kimberlitic (Mg/Ca ratios >2; >25 wt % SiO_2) 70–100°C above the solidus. For melting of model lherzolite with a CO_2 content of 0·15 wt %, this continuous change in melt composition from carbonatitic to kimberlitic takes place in the melting range 0–1%. Our data are thus consistent with an origin for group 1B kimberlites by low-degree partial melting of carbonated, garnet lherzolite at pressures of at least <10 GPa. Furthermore, the observed carbonatite–kimberlite continuum in melt compositions supports petrogenetic links between carbonatites and kimberlites in the mantle source region by small variations in the melt fraction. Carbonatites are associated with kimberlites in mobile belts adjacent to cratons, such as in the Sarfartoq region in west Greenland. Here, a continuum of rock compositions that range from kimberlite through ultramafic lamprophyres to dolomitic carbonatites is in very good agreement with the experimental data at 6 GPa, consistent with the variations in magma compositions in the Sarfartoq region being produced mainly by variations in the amount of melting at the source. Our data suggest that a similar origin may apply to other carbonatite–kimberlite–ultramafic alkaline rock associations.

KEY WORDS: *experiments*; *carbonatite*; *kimberlite*; *partial melting*; *Sarfartoq*

INTRODUCTION

Carbonatites and kimberlites have received a great deal of attention from Earth scientists for many years. For example, the widespread geographical distribution, deep-seated origin, unique geochemistry, and age span from 2·8 Ga to the present make carbonatites particularly appropriate for investigating the chemical evolution of the Earth's upper mantle through time (Bell & Blenkinsop, 1987). Kimberlites, like carbonatites, are rare, but have been found on almost every continent and are the principal transporters of mantle xenoliths that provide information on the mantle at depths in excess of 100 km. Carbonatites and kimberlites form part of a spectrum of silica-undersaturated rocks that vary widely in composition and include such rock types as melilitites, lamprophyres, and nephelinites. The petrogenesis of these rock types is, however, controversial, with disagreements over the nature and depth of the source region, whether they are primary in origin, the cause of melting (e.g. plume vs volatile fluxing), and the petrogenetic relationships among these rock types.

The mantle parentage of these various rocks is, however, without doubt and attention has focused on the role of CO_2 in melting of peridotite under upper-mantle conditions. From such experimental studies it is now well established that initial melts from carbonated lherzolite at pressures of ~3 GPa are CO_2 rich (>40 wt %) and SiO_2 poor (<10 wt %), and are thus carbonatitic in character (Wallace & Green, 1988; Thibault *et al.*, 1992;

*Corresponding author. Telephone: 972-883-6396. Fax: 972-883-2537. e-mail: dalton@utdallas.edu

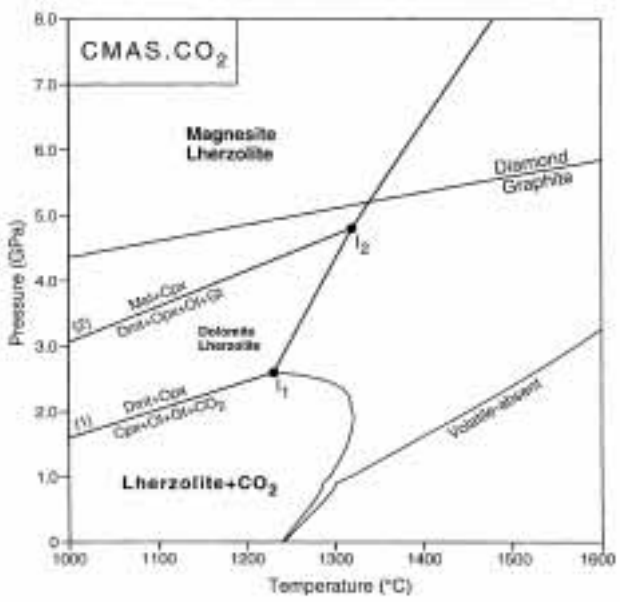

Fig. 1. Solidus of model lherzolite in the $CMAS.CO_2$ system (Dalton & Presnall, 1998). Also shown is the volatile-absent CMAS solidus from Gudfinnsson & Presnall (1996). The low-temperature cusp on both of these solidi at ~0·9 GPa results from the intersection of the subsolidus spinel lherzolite to plagioclase lherzolite transition with the solidus. Likewise, the intersection of the spinel to garnet lherzolite transition with the solidus also generates a cusp on the $CMAS.CO_2$ solidus, at ~2·1 GPa. Dmt, dolomite; Mst, magnesite; Ol, olivine; Cpx, clinopyroxene; Opx, orthopyroxene; Gt, garnet.

Dalton & Wood, 1993; Dalton & Presnall, 1998). In a recent study of phase relations in the system CaO–MgO–Al_2O_3–SiO_2–CO_2 ($CMAS.CO_2$), Dalton & Presnall (1998) determined the model lherzolite solidus (Fig. 1) and found that the solidus melts are carbonatitic to pressures of at least 7 GPa, with Ca/(Ca + Mg) ratios from 0·59 (3 GPa) to 0·45 (7 GPa). Carbonate becomes a solidus phase at I_1, causing an abrupt drop in the solidus temperature as initially determined in the CaO–MgO–SiO_2–CO_2 ($CMS.CO_2$) system by Wyllie & Huang (1976) and Eggler (1978), and also present in the $CMAS.CO_2$ system where I_1 is displaced to slightly lower pressure. A second invariant point, I_2, marks the change from dolomite-bearing to magnesite-bearing lherzolite.

Apart from the work of Dalton & Presnall (1998) and an earlier study of Canil & Scarfe (1990), there has been a dearth of phase equilibrium studies of carbonated peridotite in the diamond stability field, where some kimberlites and lamproites must originate. Furthermore, there are very few data at any pressure that indicate how melt compositions change as temperature is increased above the carbonated lherzolite solidus. To constrain the petrogenetic links that may exist among silica-undersaturated rocks in the mantle source region(s), we have determined melt compositions in equilibrium with lherzolite in the $CMAS.CO_2$ system at 6 GPa over a range of temperatures (1380–1505°C) above the carbonated lherzolite solidus (Fig. 1).

EXPERIMENTAL PROCEDURES

At 6 GPa, the solidus of model carbonated lherzolite in $CMAS.CO_2$ is an invariant point where liquid coexists with olivine, orthopyroxene, clinopyroxene, garnet and magnesite (Fig. 1). At temperatures higher than the solidus, an isobaric univariant line for the assemblage olivine + orthopyroxene + clinopyroxene + garnet + liquid extends to the CO_2-free CMAS solidus. The aim of this study was to trace the compositional path of this line and determine the compositions of coexisting phases. The advantage of this approach is that bulk compositions can be constructed that maximize the amount of liquid to facilitate analysis. As long as all five phases are present, the system remains invariant at constant temperature and pressure; and adjustments of the starting composition to increase the amount of liquid have no effect on the compositions of the coexisting phases. Thus, the compositions of liquids in equilibrium with model garnet lherzolite along this univariant curve can be readily determined.

Starting compositions were prepared from high-purity oxides and carbonates following the procedures outlined by Dalton & Presnall (1998). For each experiment, ~1 mg of the starting composition was loaded into a 1·2 mm o.d. platinum capsule that had previously been sealed at one end by arc-welding. The capsule plus starting composition was dried at 250°C for at least 24 h, weighed, welded shut and weighed again. Capsules were discarded if a weight loss of the sample of >10% resulting from decarbonation occurred during final welding. Total capsule length was 2 mm. All experiments were performed in a multianvil apparatus with 18 mm octahedra (95% MgO, 5% Cr_2O_3), WC cubes with 11 mm truncations, stepped graphite furnaces, and Al_2O_3 spacers and thermocouple sleeves. Temperatures were measured with W5%Re/W26%Re thermocouples positioned along the axis of the graphite heater and in contact with the capsule. Temperatures were automatically controlled by a Eurotherm 818 solid-state controller to within ± 1°C. On the basis of repeated determinations of the melting point of diopside at 2·5 and 5 GPa, temperature reproducibility is believed to be ± 10°C (Presnall *et al.*, 1997). Pressure calibration of the 18 mm assembly at high temperature is the same as that described by Dalton & Presnall (1997). The octahedral assembly was dried for at least 1 h at 120°C before being immediately employed in the assembly. Load was applied to the assembly until the target pressure was achieved and then temperature was raised at a rate of 100°C/min.

Table 1: Experimental conditions and results

Experiment	Temperature (°C)	Time (h)	Result
KM57	1405	6	Ol, Opx, Cpx, Gt, Lq
KM55	1430	6	Ol, Opx, Cpx, Gt, Lq
KM56	1455	6	Ol, Opx, Cpx, Gt, Lq
KM45	1480	6	Ol, Opx, Cpx, Gt, Lq
KM53	1505	6	Ol, Opx, Cpx, Gt, Lq

Ol, olivine; Gt, garnet; Lq, liquid.

ANALYTICAL PROCEDURES

At the conclusion of each experiment the entire capsule was mounted longitudinally in epoxy resin and ground under oil. Because of the fragile nature of the charge, it was necessary to vacuum-impregnate the capsule repeatedly with Petropoxy 154 resin and regrind until a satisfactory surface for diamond polishing was obtained. The compositions of the crystalline and melt phases were determined by wavelength-dispersive electron microprobe analysis using a five-spectrometer JEOL JXA 8600 Superprobe. The crystalline phases were analyzed with a focused beam using an acceleration voltage of 15 kV and a beam current of 10 nA. Standards employed were olivine (Mg), wollastonite (Ca, Si) and garnet (Al). Data were processed using the Bence–Albee matrix correction routine with the alpha coefficients of Albee & Ray (1970). At least 20 analyses of olivine, cpx, and opx, and five analyses of garnet were obtained.

The melt is composed of both quench Ca–Mg carbonates and quench silicate phases (Fig. 2). Thus, a representative analysis cannot be obtained with the analytical procedure used for the silicate phases because carbon is missing from the correction routine. Likewise, analytical routines designed specifically for carbonates (e.g. Lane & Dalton, 1994) are inadequate because of the presence of a silicate component in the melt. A routine combining these two procedures is not possible as Ca and Mg can be present in both the carbonate and silicate quench phases and stoichiometry assignment would require a knowledge of the proportion of these phases in the melt, which is, of course, unknown. Consequently, we chose to analyze the melts using the same routine as for analyzing silicates and assumed CO_2 by difference. This is not an ideal procedure but is currently the most satisfactory available. The melt was analyzed with a 15–20 μm beam using Bence–Albee matrix correction procedures. For each experiment, at least 20 analyses of the melt were obtained. Average melt compositions are presented in Table 3 (see below) and Fig. 3 (see also Table 1). Because the melt is a mixture of quench carbonate and quench silicate phases (Fig. 2b), it could be argued that analysis of the melt would give a bimodal distribution and thus the significance of presenting an average melt composition could be questioned. In Fig. 4 we plot all of the individual SiO_2 analyses for the melt in each run together with the average SiO_2 content. For each experiment we can use the data in Fig. 4 to calculate the number of analyses included by 1, 2 and 3 SD units on either side of the mean. In a normal curve, a 1 SD unit on one side of the mean taken together with the 1 SD unit on the other side of the mean accounts for ~68% of the area under the curve. For KM57, -55, -56, -45, and -53 we find this value to be 70, 62, 64, 69·5, and 71%, respectively. Likewise, the area represented by 2 SD units on either side of the mean is ~27% when the two are taken together. For KM57, -55, -56, -45, and -53 we find this value to be 23, 38, 33, 26·1, and 25·7, respectively. This analysis indicates that the distribution of analyses for SiO_2 in the melts is more or less normal, and thus the mean analysis for SiO_2 shown in Figs 3 and 4 and Table 3 is meaningful. Applying the same statistical test to the other oxides verifies this conclusion.

EXPERIMENTAL RESULTS

Table 2 gives the compositions of the silicate phases and Table 3 the composition of the melt in each experiment. No reversals were attempted to demonstrate equilibrium but the absence of zonation in the crystalline phases supports equilibrium or near-equilibrium conditions in our runs. Moreover, the high proportion of liquid in the experiments is likely to facilitate equilibration. No hydrous phases were observed in our experiments but ion probe analysis by N. Shimizu (Woods Hole Oceanographic Institution) of the liquid in runs KM14 (1380°C) and KM45 (1480°C) detected a very small amount of water, 0·31 and 0·54 wt %, respectively. These values are uncertain, however, as a basalt standard was used for calibration. Nevertheless, the results support the assessment of Canil & Scarfe (1990) that it is almost impossible to achieve truly anhydrous conditions in multi-anvil experiments when pyrophyllite is employed as a gasket material. However, given the large amount of CO_2 in these liquids (KM14, 44·6%; KM45, 18·7%) and the high proportion of liquid (~40%) in our experiments, we feel that this very small amount of water has had little, if any, effect on the phase relations.

Quench liquid occurred as a separated volume at the top of the charge ~100–200 μm deep but also interstitially between the crystalline phases (Fig. 2b). All of the liquid analyses presented in Table 3 are of the separated liquid from the top of the charge because quench modification to carbonate liquid in the vicinity of crystals can be severe (Dalton & Presnall, 1998).

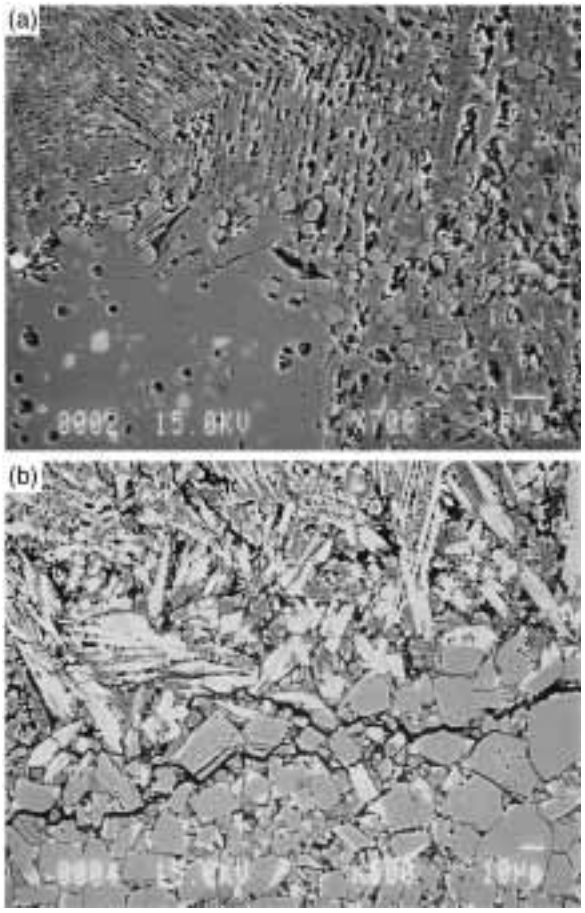

Fig. 2. Back-scattered electron micrographs of separated liquid regions in (a) KM14, at 6 GPa and 1380°C (Dalton & Presnall, 1998) and (b) KM45, at 6 GPa and 1480°C. (Note the feathery quench textures in both images and the greater proportion of quench cpx in the separated liquid in KM45.) Clinopyroxenes are the bright, almost white phase in both images. In (a) the large medium gray phase at the bottom left of the image is opx and the small (<10 μm), rounded pale gray phase scattered throughout the image is garnet. In (b) the equilibrium grains below the quench area are opx and interstitial liquid (pale gray) can be observed between these grains and is noticeably poorer in quench cpx than the separated liquid in the top half of the image. Beam conditions were 15 kV and 15 nA. The width of (a) is ~130 μm and that of (b) is ~280 μm.

Melt compositions

Compared with the solidus melt in CMAS.CO_2 at 6 GPa (Fig. 2a), the melts at temperatures above the solidus are enriched in MgO, Al_2O_3 and SiO_2, and poorer in CaO and CO_2 (Table 3). The melts are still CO_2 rich and strongly silica undersaturated, however. This can be seen in Fig. 3, where selected oxide concentrations are plotted against temperature. Of particular importance in Fig. 3 is the continuous change in the melt composition from carbonatitic at the solidus to kimberlitic at 70–100°C above the solidus. From an analysis of phase relations in the simpler CMS.CO_2 system at pressures <3 GPa, Wyllie & Huang (1975) deduced that progressive melting of carbonated peridotite would give rise to a continuum of magma compositions from carbonatitic through kimberlitic (or melilititic depending on pressure) and then to basaltic compositions at considerably higher temperatures. Our data in CMAS.CO_2 at 6 GPa experimentally confirm the carbonatite–kimberlite transition, and initial data along the isobaric univariant line involving four-phase lherzolite plus liquid at temperatures >1505°C do indeed indicate that the melt continues to change gradationally from kimberlitic towards a picritic or komatiitic composition as the CO_2-free CMAS solidus is approached.

We are aware of only one previous determination of liquid compositions in equilibrium with four-phase lherzolite in CO_2-bearing systems at pressures >4 GPa with which to compare our results. Using a natural spinel lherzolite with added CO_2 as a starting composition, Ryabchikov *et al.* (1993) determined melt compositions in equilibrium with peridotite at 5 GPa. At 1400°C, the solidus liquid in equilibrium with garnet lherzolite is carbonatitic and very similar in composition to our 5 GPa solidus melt in CMAS.CO_2 (Dalton & Presnall, 1998). With increasing temperature above the solidus, Ryabchikov *et al.* (1993) noted that the SiO_2 and MgO concentrations of the melt increase whereas the CaO concentration decreases, concordant with the present study (Fig. 3). They concluded that a liquid of kimberlitic composition would coexist with garnet lherzolite ~100–150°C above the solidus, in excellent agreement with our data (Table 3). Canil & Scarfe (1990) presented phase relations in the CMS.CO_2 system to 12 GPa but did not analyze melt compositions. Partial melt compositions calculated from mass balance at 5 and 7 GPa, however, are in relatively good agreement with our analytical data. For example, at 5 GPa and 1410°C (~120°C above their solidus) the melt in equilibrium with olivine, cpx, and opx has the composition (wt %): SiO_2, 33; CO_2, 11; MgO, 49; CaO, 7·3; and was described by Canil & Scarfe (1990) as a protokimberlite. The MgO concentration is significantly higher than in any of our melt compositions (Table 3) and higher than that of any natural kimberlite, but this may reflect underestimation of the proportion of olivine in the charge by Canil & Scarfe (1990) during their mass balance calculations. Notwithstanding this, both Canil & Scarfe (1990) and Ryabchikov *et al.* (1993) inferred from their data that kimberlites can be generated by partial melting of carbonated peridotite at pressures of 5–7 GPa. However, the continuum of melt compositions from carbonatitic to kimberlitic is demonstrated experimentally in the present study for the first time.

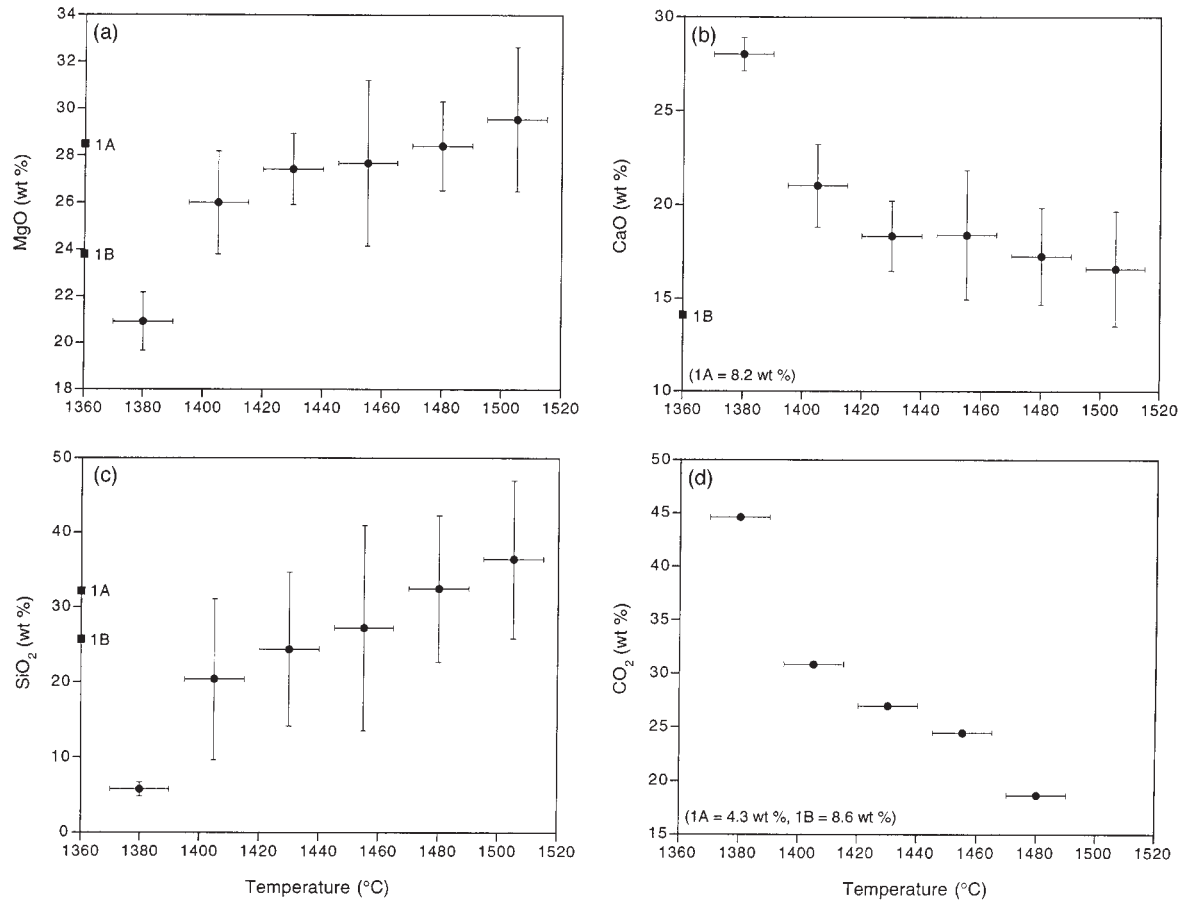

Fig. 3. Run temperature plotted against selected oxide concentrations in separated melt for the experiments detailed in Tables 1 and 3. Y error bars are 1σ. Also shown are average group 1A and 1B kimberlite compositions for these oxides from Smith *et al.* (1985).

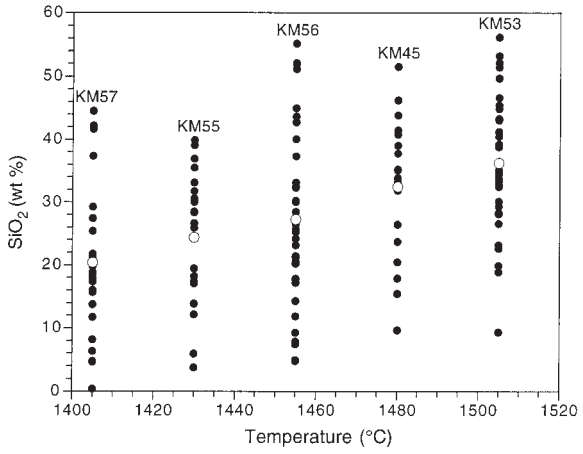

Fig. 4. Temperature vs SiO_2 (wt %). ○, average SiO_2 content of each melt from Table 3; ●, individual SiO_2 analyses of each melt.

DISCUSSION

Concerning kimberlites

Our data at 6 GPa in the CMAS.CO_2 system demonstrate that melts of kimberlitic composition are in equilibrium with garnet lherzolite at temperatures above the carbonated lherzolite solidus (KM56, -45, -53; Table 3). Specifically, these melts closely resemble the group 1B kimberlites of Smith *et al.* (1985), which have an average Mg/Ca ratio of 2·3, average SiO_2 content of 26 wt %, and are the most CO_2-rich kimberlite group, with an average content of 9 wt % (Smith *et al.*, 1985). The higher CO_2 contents of our melts compared with group 1B kimberlites may reflect some degassing of ascending kimberlite magmas, which has been experimentally demonstrated by Brey *et al.* (1991). Group 1A kimberlites are richer in SiO_2 (average 32 wt %) and poorer in CaO (average 8·2 wt %) than group 1B kimberlites, with an average Mg/Ca ratio of 4·8 (Smith *et al.*, 1985). At 1480 and 1505°C, the highest temperatures attained in this

Table 2: Mineral compositions

Experiment	CaO	MgO	Al_2O_3	SiO_2	Total
KM57 (1405°C)					
Olivine	0·13 (0·05)	56·58 (0·33)	0·04 (0·01)	43·58 (0·28)	100·34
Opx	1·28 (0·16)	38·32 (0·26)	0·77 (0·12)	59·98 (0·24)	100·35
Cpx	21·64 (0·6)	21·54 (0·43)	0·57 (0·04)	56·48 (0·33)	100·23
Garnet	5·26 (0·39)	26·25 (0·09)	24·09 (0·31)	45·27 (0·25)	100·35
KM55 (1430°C)					
Olivine	0·14 (0·03)	56·51 (0·35)	0·06 (0·03)	43·60 (0·26)	100·31
Opx	1·40 (0·10)	38·28 (0·22)	0·89 (0·1)	59·90 (0·35)	100·49
Cpx	20·51 (0·39)	22·26 (0·45)	0·67 (0·03)	56·55 (0·33)	100·00
Garnet	4·88 (0·05)	26·51 (0·22)	24·11 (0·19)	45·59 (0·01)	101·08
KM56 (1455°C)					
Olivine	0·15 (0·02)	56·43 (0·37)	0·04 (0·01)	43·49 (0·31)	100·11
Opx	1·52 (0·12)	37·83 (0·26)	0·90 (0·05)	59·95 (0·27)	100·20
Cpx	19·94 (0·23)	22·52 (0·24)	0·74 (0·03)	56·38 (0·29)	99·58
Garnet	4·83 (0·04)	26·34 (0·11)	24·36 (0·03)	45·46 (0·07)	101·00
KM45 (1480°C)					
Olivine	0·19 (0·02)	57·04 (0·39)	0·08 (0·03)	43·56 (0·39)	100·87
Opx	1·80 (0·13)	38·12 (0·15)	1·16 (0·21)	59·69 (0·2)	100·78
Cpx	19·47 (0·29)	23·40 (0·26)	0·90 (0·04)	56·62 (0·35)	100·39
Garnet	4·94 (0·08)	26·50 (0·16)	23·81 (0·3)	45·44 (0·32)	100·69
KM53 (1505°C)					
Olivine	0·19 (0·04)	56·60 (0·25)	0·15 (0·13)	43·57 (0·26)	100·51
Opx	1·82 (0·07)	37·99 (0·2)	1·10 (0·04)	59·72 (0·16)	100·63
Cpx	18·64 (0·33)	24·02 (0·37)	0·99 (0·06)	56·71 (0·35)	100·37
Garnet	4·91 (0·02)	26·60 (0·05)	24·03 (0·06)	45·27 (0·05)	100·81

Number in parentheses is 1 SD based on at least 20 spot analyses for olivine, opx, and cpx, and at least five for garnet.

Table 3: Melt compositions

Experiment	CaO	MgO	Al_2O_3	SiO_2	CO_2*	Ca/(Ca + Mg)	Mg/Ca
KM14 (1380°C)†	28·03 (0·89)	20·91 (1·25)	0·66 (0·12)	5·79 (0·93)	44·61	0·49 (0·05)	1·03
KM57 (1405°C)	21·02 (2·2)	26·00 (2·2)	1·77 (0·77)	20·37 (10·71)	30·84	0·37 (0·12)	1·72
KM55 (1430°C)	18·34 (1·87)	27·43 (1·51)	2·88 (0·69)	24·38 (10·26)	26·97	0·32 (0·11)	2·08
KM56 (1455°C)	18·40 (3·45)	27·69 (3·53)	2·21 (0·96)	27·24 (13·71)	24·46	0·32 (0·21)	2·1
KM45 (1480°C)	17·26 (2·59)	28·42 (1·9)	3·21 (0·73)	32·45 (9·8)	18·65	0·30 (0·16)	2·3
KM53 (1505°C)	16·58 (3·08)	29·57 (3·07)	3·09 (0·83)	36·23 (10·57)	14·53	0·29 (0·2)	2·48

*By difference.
†Solidus melt composition at 6 GPa from Dalton & Presnall (1998).
Number in parentheses is 1 SD based on at least 20 analyses.

study, the SiO_2 content of the melts are within the range of group 1A kimberlites but the CaO contents are much higher.

The results of the current study, together with those of Canil & Scarfe (1990) and Ryabchikov *et al.* (1993), support the earlier suggestion of Eggler & Wendlandt

(1979) from experiments on an average Lesotho kimberlite to 5·5 GPa that group 1 kimberlites can be generated by partial melting of CO_2- and H_2O-bearing garnet peridotite at pressures of ~5–8 GPa. In recent years, however, this viewpoint has been challenged, mainly because of the discovery of majorite garnet (now pyrope + exsolved pyroxene) in xenoliths and high-pressure (>400 km) mineral inclusions in diamond in a handful of kimberlites [summarized by Haggerty (1994)]. These discoveries led Ringwood *et al.* (1992) to conduct experiments on an average group 1A kimberlite at 10 and 16 GPa. The appearance of garnet well below the liquidus at 10 GPa for the studied composition indicated that kimberlite could not have been generated at pressures of 10 GPa or less, as the low concentrations of HREE in natural kimberlite require garnet to be a residual phase during partial melting. Instead, the appearance of majorite garnet as a liquidus phase at 16 GPa prompted these workers to suggest a much deeper, transition zone origin for group 1A kimberlite. The presence of garnet at 10 GPa near the liquidus of an aphanitic kimberlite (Wesselton, South Africa) studied by Edgar & Charbonneau (1993), however, led Ringwood and co-workers to repeat their 10 GPa experiments. These results have been presented by Kesson *et al.* (1994). Although they found that olivine is the liquidus phase at 10 GPa, in agreement with their earlier study, olivine was closely followed by garnet, in apparent disagreement with the earlier experiments, where garnet was reported to appear well below the liquidus. Kesson *et al.* (1994) concluded that generation of group 1A kimberlite at pressures around 10 GPa could not be ruled out, although a transition zone origin was still preferred.

Results of recent experiments conducted at 4·5–5·5 GPa using an average group 1A kimberlite by Girnis *et al.* (1995) showed that, under CO_2-saturated conditions, orthopyroxene, garnet, and magnesite were all on the liquidus in the pressure range investigated, but olivine was not a liquidus phase at pressures above 4·5 GPa. With addition of water to the experiments, however, olivine was a near-liquidus phase along with garnet and orthopyroxene. Girnis *et al.* (1995) calculated that saturation in olivine, garnet, orthopyroxene, and magnesite would occur at ~6 GPa for the composition studied. They considered generation of group 1A kimberlites by direct partial melting of magnesite-bearing garnet harzburgite at such pressures unlikely, however, because the Cr and Ti contents of the experimental garnets were not in agreement with those found in natural garnets from depleted harzburgitic xenoliths in kimberlites. Girnis *et al.* (1995) favored generation of proto-group 1A kimberlite in the lower asthenosphere or transition zone followed by interaction of these melts with strongly depleted harzburgites at the base of the continental lithosphere.

More experimental studies are required at the pressures relevant to a lower asthenosphere or transition zone origin for group 1 kimberlites before this model can be critically evaluated. Certainly, there is no reason to suppose that kimberlites cannot originate from a variety of depths within the mantle, and the presence of high-pressure inclusions in some kimberlites does require explanation. Indeed, Smith *et al.* (1985) suggested that group 1B kimberlites are generated at lower pressures than group 1A kimberlites, on the basis of geochemical differences between these two kimberlite groups and the absence of diamonds in off-craton, dominantly group 1B kimberlites. On the basis of phase equilibria constraints, Eggler (1989) came to a similar conclusion with off-craton kimberlites generated at 5 GPa, and on-craton kimberlites at 6 GPa. Our data in the CMAS.CO_2 system support an origin for group 1B kimberlites at pressures of at least <10 GPa, although generation of both group 1A and 1B kimberlites at considerably higher pressures than this cannot be precluded.

Low-degree kimberlitic melts at 6 GPa

Given an estimate of the CO_2 content of the upper mantle, we can use the data in Tables 2 and 3 to calculate the melt composition as a function of per cent melting at 6 GPa. We have done this in Fig. 5 for an upper mantle containing 0·15 wt % CO_2 (Javoy, 1997). Figure 5 shows that dramatic changes in melt composition occur over a very small melting range, with melt compositions changing continuously from carbonatitic to kimberlitic in the melting range 0–1% (1380–1505°C). Kimberlites show marked enrichment in the incompatible trace elements, implying they represent low-degree partial melts. Our data are compatible with this observation, as it is evident from Fig. 5 that melts of kimberlitic composition can be produced by as little as ~0·6–1% partial melting of carbonated garnet lherzolite at 6 GPa. For an upper mantle containing <0·15 wt % CO_2, the melt percentage required to generate a kimberlitic composition would be correspondingly smaller.

Kimberlite–carbonatite relations

Figures 3 and 5 show that melts of carbonatitic and kimberlitic composition can be produced under comparable P–T conditions by partial melting of carbonated lherzolite. Petrogenetic links between carbonatites and kimberlites are therefore implied in the CO_2-bearing mantle source region and are supported by the overlapping isotopic characteristics of carbonatites and group 1 kimberlites (Nelson *et al.*, 1988; Bell & Blenkinsop, 1989). Carbonatites are associated in space and time with kimberlites of the Pilaansberg province, Kaapval

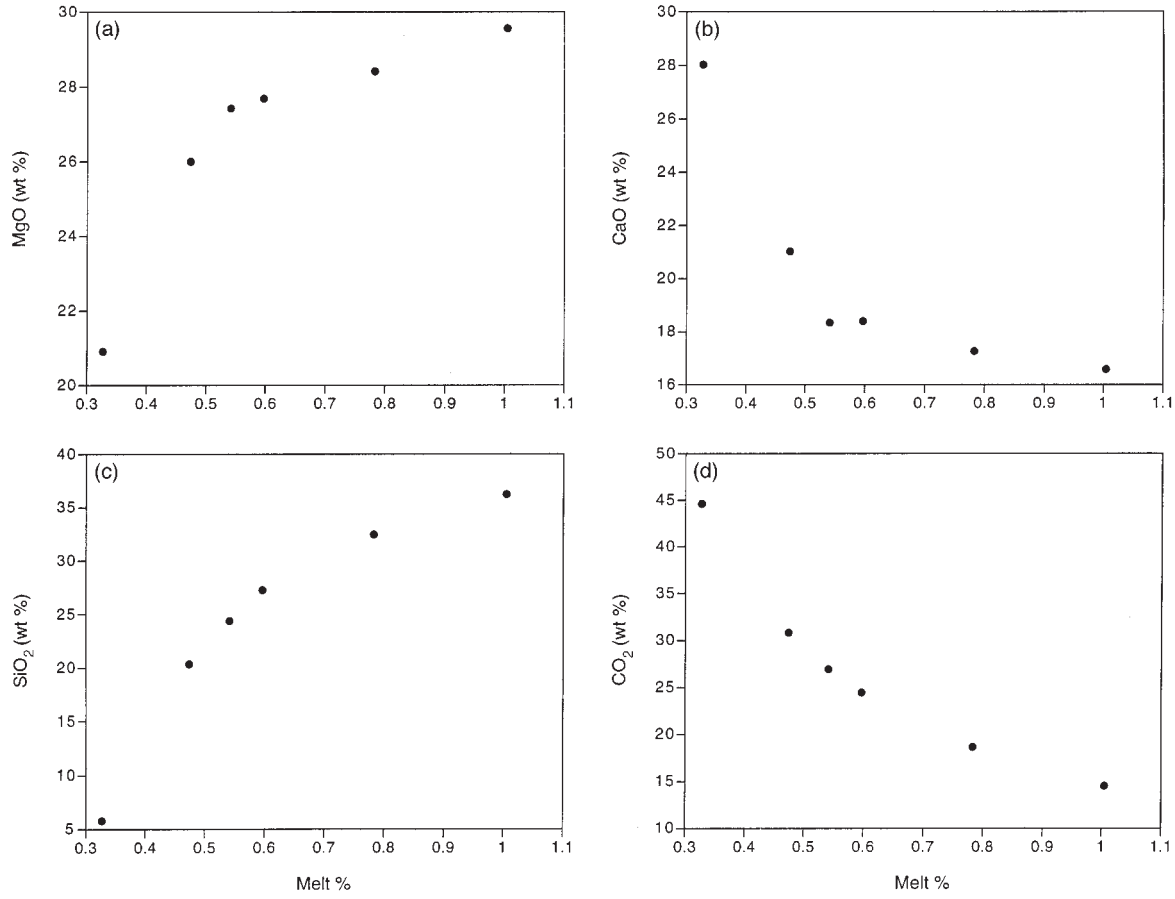

Fig. 5. Per cent melting vs oxide concentrations (wt %) for melting at 6 GPa of model lherzolite with 0·15 wt % CO_2 (Javoy, 1997).

Craton, South Africa (Dawson, 1980). (Unless otherwise stated, all subsequent use of the term kimberlite refers to group 1 kimberlites.) Also, off-craton kimberlites in circumcratonic mobile belts and fault zones can be accompanied by carbonatites (White *et al.*, 1995). Examples include the Gibeon kimberlite field in Namibia (Janse, 1975; Kurszlaukis & Lorenz, 1997), the Lucapa Corridor, Angola (White *et al.*, 1995), the Sarfartoq region, central west Greenland (Larsen & Rex, 1992), and the Halls Creek Mobile Zone, NW Australia (White *et al.*, 1995). A close spatial and temporal relationship between African carbonatites and kimberlites, particularly off-craton, was also stressed by Mitchell & Garson (1981).

Of course, an association of carbonatites and kimberlites in the same magmatic province does not necessarily imply a petrogenetic link. Given sufficient geochemical data on such provinces, it would be possible to evaluate the relationship(s) that may exist among the rock types present. Unfortunately, such chemical data on regions where carbonatites and kimberlites occur in close proximity are scant. An exception is the Sarfartoq region in central west Greenland, where a detailed geochemical data set is available on the carbonatites and kimberlites (L. M. Larsen, Geological Survey of Denmark and Greenland, unpublished data, 1997).

The Sarfartoq region, situated at the boundary between the undeformed Archean block and the Nagssugtpqidian mobile belt in central west Greenland, contains a swarm of kimberlite cone sheets centered on the Sarfartoq carbonatite intrusive complex that post-dates kimberlite emplacement (Larsen & Rex, 1992). Radiometric dating of the kimberlites and carbonatites showed them to be coeval at ~600 Ma (Larsen *et al.*, 1983). In Fig. 6, Sarfartoq carbonatite and kimberlite compositions generously provided by L. M. Larsen are plotted along with the fields for kimberlite and ultramafic lamprophyres from Rock (1991). It can be seen that there is a continuous spectrum of rock compositions from dolomitic carbonatites through to kimberlite compositions. It should be noted that the designation of carbonatites and kimberlites (by L. M. Larsen) in Fig. 6 refers to their setting within the intrusive complex (carbonatite) or outside

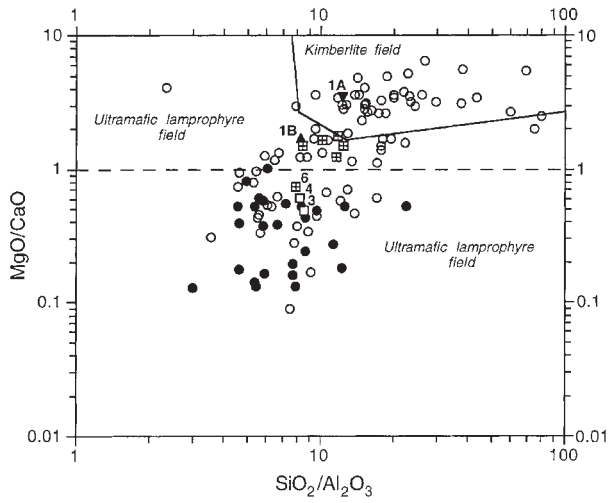

Fig. 6. Discrimination diagram for kimberlites and ultramafic lamprophyres after Rock (1991). ○, Sarfartoq kimberlites; ●, carbonatites [L. M. Larsen (unpublished data, 1997), except for nine kimberlite analyses from Scott (1977); see text for definition of carbonatite and kimberlite]. Crossed squares represent our experimental melt compositions at 6 GPa (Table 3), and open squares are solidus carbonate melts at 4 and 3 GPa taken from Dalton & Presnall (1998). Also shown are average group 1A (inverted filled triangle) and average group 1B (filled triangle) kimberlite compositions from Smith *et al.* (1985).

it (kimberlite), and not necessarily to their whole-rock chemistry. Also shown in Fig. 6 are our experimental liquids at 6 GPa (Table 3), and solidus carbonate melts in equilibrium with carbonated lherzolite at 4 and 3 GPa from our earlier work in CMAS.CO_2 (Dalton & Presnall, 1998). It is evident from Fig. 6 that the kimberlite dikes at Sarfartoq show a wide range of composition, with some samples plotting within the cluster of carbonatite analyses. Those that plot outside the carbonatite cluster, MgO/CaO ≥ 1, display a general trend in good agreement with our limited experimental melt compositions at 6 GPa (Fig. 6). We are aware of the potential pitfalls in comparing experimental melt compositions with whole-rock analyses, but we believe that comparisons act as a worthwhile tool of interpretation as long as caution is exercised. The carbonatites show no systematic variation and plot in a cluster with MgO/CaO ≤ 1 and, with one exception, SiO_2/Al_2O_3 <13.

It could be argued from Fig. 6 that fractionation is primarily responsible for the variation in kimberlite composition, and furthermore that the carbonatites at Sarfartoq are derived by fractionation from an ultramafic silicate parent magma. Certainly, there is evidence for flow differentiation within individual kimberlite dikes as discussed by Larsen & Rex (1992). Marginal facies in the wider dikes are richer in carbonate and poorer in olivine than the center of the dikes, and often mineralogically indistinguishable from the carbonatites (Larsen & Rex, 1992). In Fig. 6 these are the 'kimberlite' analyses that plot within the carbonatite cluster (MgO/CaO <1), whereas the dike centers plot outside the cluster. Although there is modal variation, the dikes display mineralogical characteristics of unevolved magmas, as discussed by Mitchell *et al.* (1998). This, together with the agreement between the experimental melts and the kimberlites with MgO/CaO >1, suggests that the kimberlites represent an array of mantle melts generated by low-degree partial melting of carbonated lherzolite at pressures >5 GPa. The range in MgO/CaO and SiO_2/Al_2O_3 ratios displayed by the kimberlites is much greater than that shown by our experimental liquids (Fig. 6). The wider range of compositions for the natural kimberlites may be due partly to the use of whole-rock analyses. Also, our data are only for a single pressure (6 GPa) and a limited temperature range above the solidus (1380–1505°C), whereas the natural kimberlites may have been generated at several pressures. A depth of generation for the Sarfartoq kimberlites of at least 5 GPa is not unreasonable, given that garnet lherzolite nodules in the kimberlite record pressures of 5·2 GPa (Larsen & Rønsbo, 1993). The deep-seated origin of these kimberlites is also supported by the finding of microdiamonds in the Sarfartoq area (Larsen & Rex, 1992).

The lack of evidence for fractionation of the kimberlites and the absence of other silicate rocks in the Sarfartoq region suggest that the carbonatites may also be primary mantle melts as proposed by Larsen & Rex (1992). Primary dolomitic carbonatites are known, for example at Rufunsa, Zambia (Bailey, 1989). Both Harmer & Gittins (1997) and Dalton & Presnall (1998) have argued that dolomitic carbonate melts could avoid decarbonation and freezing at the solidus ledge (Fig. 1) and ascend to the surface if they were out of equilibrium with the surrounding wall-rock. Dalton & Presnall (1998) showed that solidus melt compositions in the CMAS.CO_2 system were carbonatitic to at least 7 GPa, which contradicts earlier suggestions by some workers that solidus melts become kimberlitic in the magnesite stability field (Eggler, 1989). The change in MgO/CaO ratio of the solidus carbonate melt is not a strong function of pressure (Fig. 6) and does not allow us to place any real constraint on the depth of origin for the carbonatites, particularly when we are comparing simple system melts with whole-rock analyses. From a dynamic point of view, however, it is preferable to generate both the carbonatites and the kimberlites in a similar depth range. Therefore, we suggest that the Sarfartoq carbonatites are deep-seated melts that originate from pressures of at least 5 GPa.

Petrogenetic links among carbonatites, kimberlites, and ultramafic lamprophyres

A feature of Fig. 6 is that many of the Sarfartoq kimberlites considered primary in the previous discussion plot in the

ultramafic lamprophyre field of Rock (1991), as do most of our 6 GPa experimental points. Discrimination diagrams such as Fig. 6 need to be interpreted with some caution, however, given the inherently arbitrary nature of such plots. For example, the average group 1B kimberlite of Smith *et al.* (1985) plots in the ultramafic lamprophyre field in Fig. 6. Nevertheless, Fig. 6 raises the question of nomenclature and of the relationship between kimberlites, ultramafic lamprophyres, and carbonatites. The difficulty of classifying lamprophyres has been discussed by Mitchell (1994) and more recently Woolley *et al.* (1996), who could not satisfactorily classify lamprophyres and in fact suggested that aillikites (carbonate-rich ultramafic lamprophyres) may be a variety of silicio-carbonatites, carbonatites containing >10 wt % SiO_2 (Woolley & Kempe, 1989). Ultramafic lamprophyres are commonly associated with carbonatites, either as carbonatite–lamprophyre dike swarms (e.g. Kalix, Sweden, Kresten *et al.*, 1981) or in carbonatite–ijolite–nephelinite complexes such as in the alkaline complex of Fen in southern Norway (Barth & Ramberg, 1966). Both Kapustin (1981) and Rock (1991) observed that, compositionally, ultramafic lamprophyres overlap carbonatites globally and in single intrusions. Rock (1991) and Bailey (1993) stressed the importance of the carbonatite–ultramafic lamprophyre relationship, echoing Le Bas (1977), who suggested that ultramafic lamprophyres provide the link between carbonatite–nephelinite and kimberlite magmatism. Globally, there is a compositional continuum between carbonatites, ultramafic lamprophyres, and kimberlites (Rock, 1991).

It is tempting to take such observations and construct petrogenetic links among these rock types. This is particularly enticing given our experimental data, which show that progressive partial melting of carbonated lherzolite produces carbonatitic to kimberlitic melts with intermediary compositions not unlike ultramafic lamprophyres [average aillikite Mg/Ca, 1·2; CO_2, 9·6 wt %, from Rock (1991)]. For the Sarfartoq region, we have indeed advocated partial melting as the most important factor determining magma composition, and that petrogenetic links between the rock types present are established in the mantle source region. At Sarfartoq, ultramafic lamprophyres and kimberlites are an integral part of the magmatism together with carbonatites. Whether Sarfartoq is representative of other regions where kimberlites and/or ultramafic lamprophyres occur with carbonatites and nephelinitic rock types are absent cannot be constrained by available data. Not only is a detailed geological knowledge of such localities required, but also criteria for distinguishing primary from derivative carbonate-rich magmas such as that attempted by Eggler (1989). There can be no question, though, that very small differences in the amount of melting of carbonated mantle at 6 GPa produce strong compositional variations in the melts, and that this process, if applicable over a range of pressures, may be the crucial factor in determining the great variety of strongly silica-undersaturated melts emplaced in the crust. Although much work is required to substantiate this proposition, the importance of partial melting is highlighted by recent isotopic data from East African carbonatite–nephelinite centers, which suggest that individual nephelinitic flows at such centers represent discrete, low-volume, partial mantle melts (Bell & Peterson, 1991; Simonetti & Bell, 1995).

ACKNOWLEDGEMENTS

We are deeply indebted to Lotte M. Larsen of the Geological Survey of Denmark and Greenland for providing us with her unpublished Sarfartoq data set and for many discussions pertaining to this locality. Tim Dennison is thanked for many useful discussions concerning lamprophyres, Dr Stephan Kurszlaukis for reprints and preprints of his work on Gross Brukkaros, and Keith Bell, David Eggler, Woh-jer Lee, Bob Luth, and Peter Wyllie for constructive reviews of the manuscript. We also thank Nobu Shimizu for performing ion probe analysis of our run products at short notice, and Keith Bell for editorial patience. This research was supported by Texas Advanced Research Program Grants 009741-044 and 009741-0046 and National Science Foundation Grants EAR-9219159 and EAR-9725900. This paper is Contribution 874 of the Department of Geosciences, University of Texas at Dallas.

REFERENCES

Albee, A. L. & Ray, L. (1970). Correction factors for electron-probe microanalysis of silicates, oxides, carbonates, and sulphates. *Analytical Chemistry* **42,** 1408–1414.

Bailey, D. K. (1989). Carbonate melt from the mantle in the volcanoes of south-east Zambia. *Nature* **388,** 415–418.

Bailey, D. K. (1993). Carbonate magmas. *Journal of the Geological Society, London* **150,** 637–651.

Barth, T. F. W. & Ramberg, I. B. (1966). The Fen circular complex. In: Tuttle, O. F. & Gittins, J. (eds) *Carbonatites*. New York: John Wiley, pp. 225–260.

Bell, K. & Blenkinsop, J. (1987). Archean depleted mantle—evidence from Nd and Sr initial isotopic ratios of carbonatites. *Geochimica et Cosmochimica Acta* **51,** 291–298.

Bell, K. & Blenkinsop, J. (1989). Neodymium and strontium isotope geochemistry of carbonatites. In: Bell, K. (ed.) *Carbonatites: Genesis and Evolution*. London: Unwin Hyman, pp. 278–300.

Bell, K. & Peterson, T. (1991). Nd and Sr isotope systematics of Shombole volcano, East Africa, and the links between nephelinites, phonolites, and carbonatites. *Geology* **19,** 582–585.

Brey, G. P., Kogarko, L. N. & Ryabchikov, I. D. (1991). Carbon dioxide in kimberlitic melts. *Neues Jahrbuch für Mineralogie, Monatshefte* **4,** 159–168.

Canil, D. & Scarfe, C. M. (1990). Phase relations in peridotite + CO_2 systems to 12 GPa: implications for the origin of kimberlite and

carbonate stability in the Earth's upper mantle. *Journal of Geophysical Research* **95,** 15805–15816.

Dalton, J. A. & Presnall, D. C. (1997). No liquid immiscibility in the system $MgSiO_3$–SiO_2 at 5·0 GPa. *Geochimica et Cosmochimica Acta* **61,** 2367–2373.

Dalton, J. A. & Presnall, D. C. (1998). Carbonatitic melts along the solidus of model lherzolite in the system CaO–MgO–Al_2O_3–SiO_2–CO_2 from 3 to 7 GPa. *Contributions to Mineralogy and Petrology* **131,** 123–135.

Dalton, J. A. & Wood, B. J. (1993). The compositions of primary carbonate melts and their evolution through wallrock reaction in the mantle. *Earth and Planetary Science Letters* **119,** 511–525.

Dawson, J. B. (1980). *Kimberlites and their Xenoliths*. Berlin: Springer-Verlag.

Edgar, A. D. & Charbonneau, H. E. (1993). Melting experiments on a SiO_2-poor, CaO-rich aphanitic kimberlite from 5–10 GPa and their bearing on sources of kimberlite magmas. *American Mineralogist* **78,** 132–142.

Eggler, D. H. (1978). The effect of CO_2 upon partial melting of peridotite in the system Na_2O–CaO–Al_2O_3–MgO–SiO_2–CO_2 to 35 kb, with an analysis of melting in a peridotite–H_2O–CO_2 system. *American Journal of Science* **278,** 305–343.

Eggler, D. H. (1989). Carbonatites, primary melts, and mantle dynamics. In: Bell, K. (ed.) *Carbonatites: Genesis and Evolution*. London: Unwin Hyman, pp. 561–579.

Eggler, D. H. & Wendlandt, R. F. (1979). Experimental studies on the relationship between kimberlite magmas and partial melting of peridotite. In: Boyd, F. R. & Meyer, H. O. A. (eds) *Kimberlites, Diatremes and Diamonds: their Geology, Petrology, and Geochemistry*. Washington, DC: American Geophysical Union, pp. 330–338.

Girnis, A. V., Brey, G. P. & Ryabchikov, I. D. (1995). Origin of Group 1A kimberlites: fluid-saturated melting experiments at 45–55 kbar. *Earth and Planetary Science Letters* **134,** 283–296.

Gudfinnsson, G. H. & Presnall, D. C. (1996). Melting relations of model lherzolite in the system CaO–MgO–Al_2O_3–SiO_2 at 2·4–3·4 GPa and the generation of komatiites. *Journal of Geophysical Research* **101,** 27701–27709.

Haggerty, S. E. (1994). Superkimberlites: a geodynamic diamond window to the Earth's core. *Earth and Planetary Science Letters* **122,** 57–69.

Harmer, R. E. & Gittins, J. (1997). Dolomitic carbonatite parental magmas. *Proceedings of the 50th Geological Association of Canada–Mineralogical Association of Canada Annual Meeting* **22,** 64.

Janse, A. J. A. (1975). Kimberlite and related rocks from the Nama Plateau of south-west Africa. *Physics and Chemistry of the Earth* **9,** 81–94.

Javoy, M. (1997). The major volatile elements of the Earth: their origin, behavior, and fate. *Geophysical Research Letters* **24,** 177–180.

Kapustin, Y. L. (1981). Damkjernites—dike equivalents of carbonatites. *International Geology Review* **23,** 1326–1334.

Kesson, S. E., Ringwood, A. E. & Hibberson, W. O. (1994). Kimberlite melting relations revisited. *Earth and Planetary Science Letters* **121,** 261–262.

Kresten, P., Åhman, E. & Brunfelt, A. O. (1981). Alkaline ultramafic lamprophyres and associated carbonatite dykes from the Kalix area, northern Sweden. *Geologische Rundschau* **70,** 1215–1231.

Kurszlaukis, S. & Lorenz, V. (1997). Volcanological features of a low-viscosity melt: the carbonatitic Gross Brukkaros volcanic field, Namibia. *Bulletin of Volcanology* **58,** 421–431.

Lane, S. J. & Dalton, J. A. (1994). Electron microprobe analysis of geological carbonates. *American Mineralogist* **79,** 745–749.

Larsen, L. M. & Rex, D. C. (1992). A review of the 2500 Ma span of alkaline–ultramafic, potassic and carbonatitic magmatism in West Greenland. *Lithos* **28,** 367–402.

Larsen, L. M. & Rønsbo, J. (1993). Conditions of origin of kimberlites in West Greenland: new evidence from the Sarfartoq and Sukkertoppen regions. *Rapport Grønlands Geologiske Undersøgelse* **159,** 115–120.

Larsen, L. M., Rex, D. C. & Secher, K. (1983). The age of carbonatites, kimberlites and lamprophyres from southern West Greenland: recurrent alkaline magmatism during 2500 million years. *Lithos* **16,** 215–221.

Le Bas, M. J. (1977). *Carbonatite–Nephelinite Volcanism*. London: John Wiley.

Mitchell, A. H. G. & Garson, M. S. (1981). *Mineral Deposits and Global Tectonic Settings*. London: Academic Press.

Mitchell, R. H. (1994). Suggestions for revisions to the terminology of kimberlites and lamprophyres from a genetic viewpoint. In: Meyer, H. O. A. & Leonardos, O. H. (eds) *Kimberlites, Related Rocks, and Mantle Xenoliths. Proceedings of the Fifth International Kimberlite Conference, 1*. Rio de Janeiro: Companhia de Pesquisa de Recursos Minerais, pp. 15–26.

Mitchell, R. H., Scott Smith, B. H. & Larsen, L. M. (1998). Mineralogy of ultramafic dikes from the Sarfartoq, Sisimiut and Maniitsoq areas, west Greenland: kimberlites or melnoites? *Extended Abstracts, Seventh International Kimberlite Conference, Cape Town*. Cape Town: University of Cape Town, pp. 600–602.

Nelson, D. R., Chivas, A. R., Chappell, B. W. & McCulloch, M. T. (1988). Geochemical and isotopic systematics in carbonatites and implications for the evolution of ocean-island sources. *Geochimica et Cosmochimica Acta* **52,** 1–17.

Presnall, D. C., Dalton, J. A., Weng, Y.-H., Yale, L. B. & Morris, K. J. (1997). Temperature–pressure precision of multianvil experiments at pressures <7 GPa. *First International Pressure Calibration Conference, 1*. Misasa: Institute for the Study of the Earth's Interior, Okayama University, p. 15.

Ringwood, A. E., Kesson, S. E., Hibberson, W. & Ware, N. (1992). Origin of kimberlites and related magmas. *Earth and Planetary Science Letters* **113,** 521–538.

Rock, N. M. S. (1991). *Lamprophyres*. Glasgow: Blackie.

Ryabchikov, I. D., Brey, G. P. & Bulatov, V. K. (1993). Carbonate melts coexisting with mantle peridotites at 50 kbar. *Petrology* **1,** 189–194.

Scott, B. H. (1977). Petrogenesis of kimberlites and associated potassic lamprophyres from Central West Greenland. Ph.D. Thesis, University of Edinburgh.

Simonetti, A. & Bell, K. (1995). Nd, Pb and Sr isotopic data from the Mount Elgon volcano, eastern Uganda–western Kenya: implications for the origin and evolution of nephelinite lavas. *Lithos* **36,** 141–153.

Smith, C. B., Gurney, J. J., Skinner, E. M. W., Clement, C. R. & Ebrahim, N. (1985). Geochemical character of southern Africa kimberlites; a new approach based on isotopic constraints. *Transactions of the Geological Society of South Africa* **88,** 267–280.

Thibault, Y., Edgar, A. D. & Lloyd, F. E. (1992). Experimental investigation of melts from a carbonated phlogopite lherzolite: implications for metasomatism in the continental lithospheric mantle. *American Mineralogist* **77,** 784–794.

Wallace, M. E. & Green, D. H. (1988). An experimental determination of primary carbonatite magma composition. *Nature* **335,** 343–346.

White, S. H., de Boorder, H. & Smith, C. B. (1995). Structural controls of kimberlite and lamproite emplacement. *Journal of Geochemical Exploration* **53,** 245–264.

Woolley, A. R. & Kempe, D. R. C. (1989). Carbonatites: nomenclature, average chemical compositions, and element distribution. In: Bell, K. (ed.) *Carbonatites: Genesis and Evolution*. London: Unwin Hyman, pp. 1–14.

Woolley, A. R., Bergman, S. C., Edgar, A. D., Mitchell, R. H., Rock, N. M. S. & Scott-Smith, B. H. (1996). Classification of lamprophyres,

lamproites, kimberlites, and the kalsilitic, melilitic, and leucitic rocks. *Canadian Mineralogist* **34,** 175–186.

Wyllie, P. J. & Huang, W.-L. (1975). Peridotite, kimberlite, and carbonatite explained in the system CaO–MgO–SiO_2–CO_2. *Geology* **3,** 621–624.

Wyllie, P. J. & Huang, W.-L. (1976). Carbonation and melting reactions in the system CaO–MgO–SiO_2–CO_2 at mantle pressures with geophysical and petrological applications. *Contributions to Mineralogy and Petrology* **54,** 79–107.